JOURNAL OF OPTOELECTRONICS AND ADVANCED MATERIALS Vol. 9, No. 11, November 2007, p. 3619 - 3623

# The synthesis and characteristics of erbium$_{(x)}$ytterbium$_{(1-x)}$ bis(2-ethylhexyl)phosphate]$_3$

G. WANG*, M. ZHAO, Y. GU, S. ZHOU
*Photonics Research Center, School of Physics and Optoelectronic Engineering, Dalian University of Technology, Dalian, Liaoning, 116024, China*

Erbium$_{(x)}$ytterbium$_{(1-x)}$[bis(2-ethylhexyl)phosphate]$_3$ with various concentrations of Er (x) and Yb (1-x) were synthesized. The C and H contents of the complexes were determined by elemental analysis, and the concentrations of Er and Yb were measured by ICP-AES. The chemical structure and thermal stability of the complexes were investigated by FT-IR, XRD and TGA. The results indicate that all Erbium$_{(x)}$ytterbium$_{(1-x)}$[bis(2-ethylhexyl)phosphate]$_3$ have the same chemical structure. The chemical formula of the complexes is in agreement with $Er_xYb_{(1-x)}[(C_8H_{17}O)_2PO_2]_3$. The TG measurement suggests that the complexes have a good thermal stability, and there is no weight loss up to 300 ℃. The photoluminescence spectra were recorded and analyzed. When the concentration of $Er^{3+}$ ions (x) is equal to 0.107, the photoluminescence intensity of the material reaches maximum.

(Received July 3, 2007; accepted November 1, 2007)

*Keywords:* Erbium, Ytterbium, bis(2-ethylhexyl) phosphate, Thermal stability, Photoluminescence

## 1. Introduction

Er-doped polymer materials are under intensive research because of their potential applications to optoelectronic devices [1-5]. Polymer materials would have advantages over inorganic materials in devices, because fabrication and integration of polymer waveguide-based optical components is relatively easy with standard lithographic techniques [6-8]. The trivalent state $Er^{3+}$ shows an intra-4*f* transition from its first excited state ($^4I_{13/2}$) to the ground state ($^4I_{15/2}$), which occurs at a wavelength of at 1550 nm (one of the standard telecommunication wavelengths), belongs to the maximum transparency window. These feature make Er-doped polymer materials very attractive for lasers and optical amplifiers operating at 1550 nm [9,10].

In order to enhance 1550 nm gain performances of the corresponding materials and devices, an important issue towards further optimization of IR emission in Er-doped materials is the use of adequately chosen sensitizers (usually other lanthanide ions) [11,12]. Codoping with $Yb^{3+}$ can enhance greatly the photoluminescence (PL) intensity of $Er^{3+}$, owning to the energy transfer from the $Yb^{3+}$– $^2F_{5/2}$ to the $Er^{3+}$–$^2I_{11/2}$ state [13-15]. The PL efficiency is greatly improved, because the absorption cross section of $Yb^{3+}$ ions in the range from 850 to 1000nm is much larger than that of $Er^{3+}$ ions [16,17].

Early in the 1960s, the rare earth metal ions with the organophosphorus compounds were studied extensively because of their polymeric structure and properties.[18-20]. Now, some organophosphorus complexes have been utilized widely as extractant for the rare earth metal ions [21,22]. However, to our knowledge, the investigation on the structure and properties of the Erbium$_{(x)}$ytterbium$_{(1-x)}$[bis(2-ethylhexyl)phosphate]$_3$ ($Er_xYb_{(1-x)}(DIOP)_3$) has not been reported. In the present work, we synthesized $Er(DIOP)_3$, $Yb(DIOP)_3$ and $Er_xYb_{(1-x)}(DIOP)_3$ with various ratios of concentrations of Er and Yb, determined the optimum ratio of Er to Yb contents for obtaining the maximum PL intensity at constant common concentration of both metals and investigated the structure and thermal properties of these complexes.

## 2. Experimental

### 2.1 Materials

Hydrated erbium chloride ($ErCl_3·6H_2O$) (99.995%) and hydrated ytterbium chloride ($YbCl_3·6H_2O$) (99.99%) were purchased from Shandong yutai qingda fine chemical plant, China. Bis(2-ethylhexyl) phosphate (Chemical pure) was purchased from Tianjin Guangfu fine chemical research institute, China. Other reagents were analytical grade and used without further purification.

### 2.2 Synthesis of $Er(DIOP)_3$, $Yb(DIOP)_3$ and $Er_xYb_{(1-x)}(DIOP)_3$

$Er(DIOP)_3$, $Yb(DIOP)_3$ and $Er_xYb_{(1-x)}(DIOP)_3$ with various concentrations of Er and Yb were synthesized by suspending $ErCl_3·6H_2O$ and $YbCl_3·6H_2O$ in excess of

bis(2-ethylhexyl) phosphate under ambient temperature, and the temperature of the mixture was raised at a rate of 1 ~ 2℃ per min with continuously stirring. $ErCl_3 \cdot 6H_2O$ and $YbCl_3 \cdot 6H_2O$ gradually dissolved in bis(2-ethylhexyl) phosphate. Heating was continued until white precipitate was observed, and the temperature of the mixture was maintained at this level for 5 min in order to complete the precipitation. The solid precipitate was separated by filtration and washed several times with acetone, then dried in vacuum oven.

### 2.3 Characterization

Elemental analysis was carried out on Vario EL III (Elementar Analyaenaysteme GmbH, Germany) to determine the C and H contents in the samples. The concentrations of Er and Yb in the samples were determined by a Perkin-Elmer Optima 2000DV inductively coupled plasma-atomic emission spectroscopy (ICP-AES) instrument. The infrared absorption spectra were recorded on a Thermo Nicolet Nexus Euro Fourier transform infrared (FTIR) spectrometer. Samples were examined in the 400-4000 $cm^{-1}$ and 50–400 $cm^{-1}$ regions by using the KBr pellet and polytetrafluoroethylene pellet methods, respectively. The Raman spectra were measured by using a Raman spectrometer (Renishaw invia, UK) at room temperature. The 632.8 nm line from He–Ne laser was used to excite the samples with a power of 35 mW. The crystalline structure of the samples was examined on a Shimadzu XRD-6000 X-ray diffractometer (XRD) with CuKa radiation. Thermogravimetric analysis(TGA) was carried out with a Mettler Toledo TGA/SDTA 851 thermogravimetric analyzer, at a heating rate of 10 ℃ $min^{-1}$ up to 500 ℃ in $N_2$ atmosphere. The near-infrared PL characteristic was performed at room temperature by exciting at 980 nm from a semiconductor laser and by detecting with a semiconductor-cooled InGaAs detector. Powder samples in the 1mm thick cuvette were used for measurements by transmission. The experimental apparatus are shown in Fig 1.

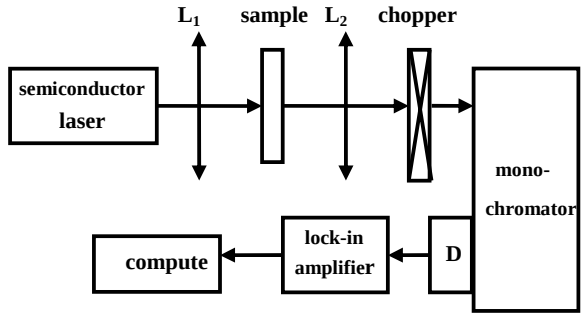


***L₁ and L₂*: Convergent lenses *D*: Detector**

*Fig. 1. The photoluminescence measurement apparatus.*

## 3. Results and discussion

To investigate the structure and thermal stability of the $Er_xYb_{(1-x)}(DIOP)_3$, the complexes with various concentrations of doping erbium were measured by FTIR spectra, Raman spectra, XRD and TGA. Because the curves of all samples with different concentrations of erbium were pretty similar, here only the data on the sample with x = 0.072 were present and discussed in detail.

### 3.1 Composition of $Er(DIOP)_3$, $Yb(DIOP)_3$ and $Er_xYb_{(1-x)}(DIOP)_3$

The C and H concentrations of $Er(DIOP)_3$, $Yb(DIOP)_3$ and $Er_xYb_{(1-x)}(DIOP)_3$ were determined by elemental analysis, and the concentrations of Er and Yb were measured by ICP-AES. The results are shown in Table 1. It can be seen that the contents of C, H, Er and Yb from practical measurement are very approximate to the theoretical value calculated from the chemical formula $Er_xYb_{(1-x)}[(C_8H_{17}O)_2PO_2]_3$. This indicates that the composition of $Er_xYb_{(1-x)}(DIOP)_3$ is in agreement with the chemical formula $Er_xYb_{(1-x)}[(C_8H_{17}O)_2PO_2]_3$.

*Table 1. The concentrations of C, H, Er and Yb for $Er(DIOP)_3$, $Er_xYb_{(1-x)}(DIOP)_3$ and $Yb(DIOP)_3$.*

| complex | C / wt% | H / wt% | Er / wt% | Yb / wt% |
|---|---|---|---|---|
| a | 50.74 (50.97) | 9.00 (9.03) | 15.23 (14.78) | 0 |
| e | 50.10 (50.72) | 8.99 (8.98) | 1.06 (0.99) | 14.66 (14.21) |
| f | 49.71 (50.70) | 8.91 (8.98) | 0 | 15.64 (15.23) |

the values in the brackets are from the theoretical calculation.

The various concentrations of Er and Yb in $Er(DIOP)_3$, $Yb(DIOP)_3$ and $Er_xYb_{(1-x)}(DIOP)_3$ are shown in Table 2. From Table 2 it can be seen that the total concentrations of Er and Yb are from 15.15 wt% to 15.91 wt%. The theoretical values of the Er and Yb total concentrations in the complexes are about 15 wt%, there is a good correlation between the experimental and theoretical data. It is an evidence that the structure of $Er_xYb_{(1-x)}(DIOP)_3$ is compatible with that of $Er(DIOP)_3$ and $Yb(DIOP)_3$ by the similar chemical reactivity. The x – values reflecting the concentrations of erbium are also shown in Table 2.

*Table 2 The concentrations of Er and Yb for Er(DIOP)$_3$, Er$_x$Yb$_{(1-x)}$(DIOP)$_3$ and Yb(DIOP)$_3$.*

| Complex | $Er^{3+}$ content / wt % | $Yb^{3+}$ content / wt % | $Er^{3+}$ and $Yb^{3+}$ content / wt % | x |
|---|---|---|---|---|
| a | 15.23 | 0 | 15.23 | 1 |
| b | 4.53 | 11.38 | 15.91 | 0.308 |
| c | 1.87 | 13.94 | 15.81 | 0.127 |
| d | 1.57 | 13.58 | 15.15 | 0.107 |
| e | 1.06 | 14.66 | 15.72 | 0.072 |
| f | 0 | 15.64 | 15.64 | 0 |

### 3.1 FTIR spectra

Fig. 2 shows the FTIR spectra of the bis(2-ethylhexyl) phosphate, Er(DIOP)$_3$, Yb(DIOP)$_3$ and Er$_x$Yb$_{(1-x)}$(DIOP)$_3$ in the 400–4000 cm$^{-1}$ region. It can be seen that the main bands of the bis(2-ethylhexyl) phosphate in this region were assigned as follows (curve g): near 1033 cm$^{-1}$ (C-O (P) stretching), 1228 cm$^{-1}$ (P=O stretching), 2327 cm$^{-1}$ ((P) OH stretching), 2900 cm$^{-1}$ ($CH_2$ and $CH_3$ stretching) and 1463 cm$^{-1}$ ($CH_2$ and $CH_3$ bending). But from the spectra of Er(DIOP)$_3$, Er$_x$Yb$_{(1-x)}$(DIOP)$_3$ and Yb(DIOP)$_3$ (curves a, e and f) we can see that the band at 1228 cm$^{-1}$ disappeared, and replaced by two new absorption bands at 1180 cm$^{-1}$ and 1106 cm$^{-1}$ (O-P-O stretching, symmetric and asymmetric). Meanwhile, the absorption band at 2327 cm$^{-1}$ disappeared.

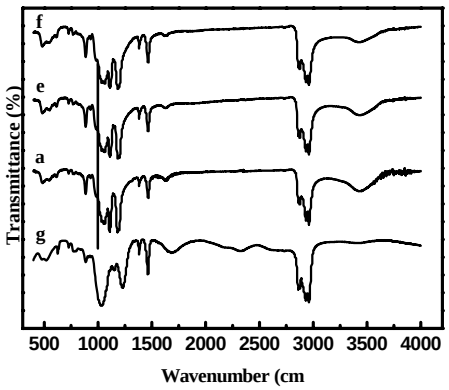


*Fig. 2 FTIR spectra in the 400–4000 cm$^{-1}$ region of: (a) Er(DIOP)$_3$ (e) Er$_x$Yb$_{(1-x)}$(DIOP)$_3$ (f) Yb(DIOP)$_3$ (g) bis(2-ethylhexyl) phosphate*

The Raman spectra of Er$_x$Yb$_{(1-x)}$(DIOP)$_3$ are shown in Fig. 3. Compared to the bands of IR spectrum in Fig. 2 (curve e) at 1060, 1180, 1463, 2870, and 2960 cm$^{-1}$, there are coincidences for the bands observed in the Raman spectrum at 1068, 1149, 1450, 2875 and 2937 cm$^{-1}$.

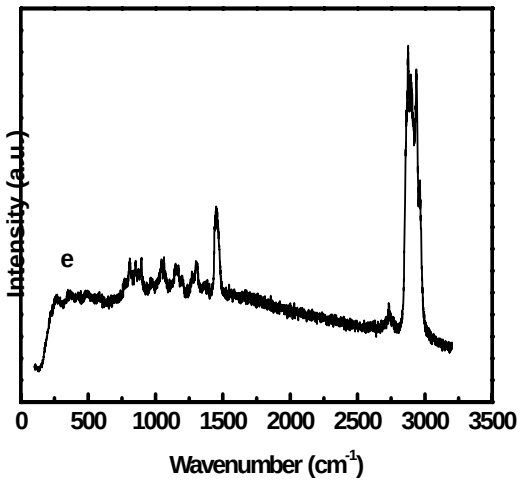


*Fig. 3 Raman spectra of Er$_x$Yb$_{(1-x)}$(DIOP)$_3$*

The FTIR spectra in the 50–400 cm$^{-1}$ region are shown in Fig. 4. Apparently, the strong bands at 204 cm$^{-1}$ occur invariably in the Er(DIOP)$_3$, Er$_x$Yb$_{(1-x)}$(DIOP)$_3$ and Yb(DIOP)$_3$ (curves a, e and f). But the spectrum of bis(2-ethylhexyl) phosphate do not exhibit the absorption in the band (curve g). Absorption at 204 cm$^{-1}$ is attributed to the Er (Yb)-O vibrations. These characters of the complexes in IR spectra indicate sufficiently that the $Er^{3+}$ and $Yb^{3+}$ have coordinated to the bis(2-ethylhexyl) phosphate. From Fig. 2 and Fig. 4 it can also be seen that Er(DIOP)$_3$, Er$_x$Yb$_{(1-x)}$(DIOP)$_3$ and Yb(DIOP)$_3$ have similar IR spectra. This reveals that these complexes are of the same chemical structure.

In addition, the spectra of the complexes show the characteristic absorption bands near 3400 cm$^{-1}$ ($H_2O$ stretching). These suggest the existing of crystal water in the complexes. But in the next thermogravimetric analysis of the complexes there is no weight loss stage of crystal water. Therefore, the band near 3400 cm$^{-1}$ is from the water absorbed by KBr in measuring.

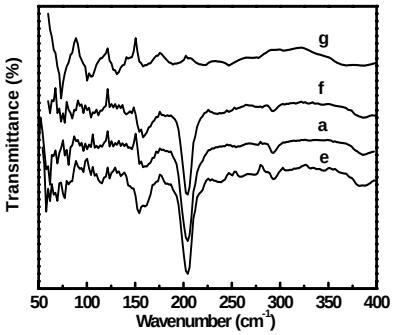


*Fig. 4 FTIR spectra in the 50–400 cm$^{-1}$ region of: (a) Er(DIOP)$_3$ (e) Er$_x$Yb$_{(1-x)}$(DIOP)$_3$ (f) Yb(DIOP)$_3$ (g) bis(2-ethylhexyl) phosphate*

### 3.2 X-ray diffraction

Fig. 5 shows XRD patterns of Er(DIOP)$_3$, Er$_x$Yb$_{(1-x)}$(DIOP)$_3$ and Yb(DIOP)$_3$. It can be seen that all the complexes exhibit the similar XRD pattern. This suggests that Er(DIOP)$_3$, Er$_x$Yb$_{(1-x)}$(DIOP)$_3$ and Yb(DIOP)$_3$ have the same crystalline structure. This pattern matches perfectly with the JCPDS (00-049-1919 ). No peak of any other phase was detected. With decreasing the concentration of $Er^{3+}$, and increasing the concentration of $Yb^{3+}$ in the complexes, the diffraction peaks had no distinct shift. The explanation for this result is that $Er^{3+}$ and $Yb^{3+}$ have the similar ionic radii of 1.00Å and 0.99 Å. The rare earth metal ions with the organophosphorus compounds have been studied extensively, and their polymeric structure has been confirmed by L. M. Li and N. M. Karayannis etc [18-20]. The results from FTIR spectra and XRD patterns demonstrate that Er(DIOP)$_3$, Er$_x$Yb$_{(1-x)}$(DIOP)$_3$ and Yb(DIOP)$_3$ have the same polymeric structure.

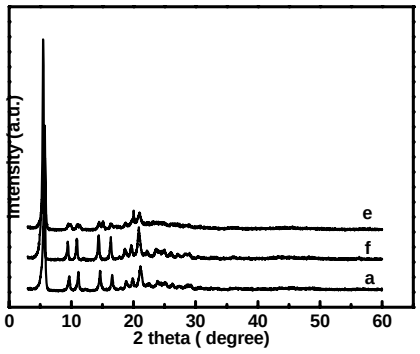


*Fig. 5. XRD patterns of: (a) Er(DIOP)$_3$ (e) Er$_x$Yb$_{(1-x)}$(DIOP)$_3$ and (f) Yb(DIOP)$_3$*

### 3.3 Thermogravimetric analyses

Fig. 6 shows the variation of the thermogravimetric curves for Er(DIOP)$_3$, Yb(DIOP)$_3$ and Er$_x$Yb$_{(1-x)}$(DIOP)$_3$. From the thermogravimetric curves it can be seen that all the complexes present a relative good thermostability since no weight loss occurred until 300 ℃. The decomposition temperature range of the complexes is from about 300 ℃ to 340 ℃. From the TGA curves we can also see that all the complexes demonstrate the same weight loss process. Only one degradation stage are observed. These suggest that the decomposition of these complexes is finished only once. No the stage of water loss is observed from Fig. 6, which reveals there is no crystal water in the complexes. For the Er(DIOP)$_3$, the weight loss is about 65%. When $Er^{3+}$ is replaced by $Yb^{3+}$ in the complexes, the weight loss is a little lower. This is a reasonable suggestion, because the atomic weight of Yb is slightly larger than that of Er.

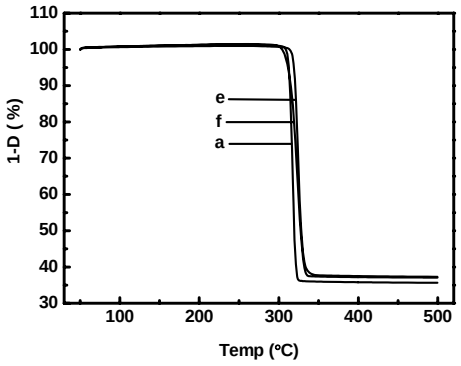


*Fig. 6. TGA curves of: (a) Er(DIOP)$_3$ (e) Er$_x$Yb$_{(1-x)}$(DIOP)$_3$ and (f) Yb(DIOP)$_3$*

The maximum weight loss temperature of Er(DIOP)$_3$, Yb(DIOP)$_3$ and Er$_x$Yb$_{(1-x)}$(DIOP)$_3$ with various concentrations of Er and Yb are summarized in Table 3. The weight loss temperature of Er(DIOP)$_3$ and Yb(DIOP)$_3$ are separately 312℃ and 319℃. From Table 3 it can be seen that with increasing the concentration of Yb in the complexes, the weight loss temperature is slightly higher.

*Table 3 The maximum weight loss temperature of Er(DIOP)$_3$, Yb(DIOP)$_3$ and Er$_x$Yb$_{(1-x)}$(DIOP)$_3$.*

| Samples | a | b | c | d | e | f |
|---|---|---|---|---|---|---|
| maximum weight loss temperature (℃) | 312 | 313 | 315 | 315 | 319 | 319 |

### 3.4 Photoluminescence(PL) spectrum

Fig. 7 displays the PL spectra of Er(DIOP)$_3$ and $Er_xYb_{(1-x)}(DIOP)_3$ with various concentrations of Er and Yb, pumped by a 980-nm diode laser at the room-temperature. It can be seen that the PL spectra reflect the typical features of the transition of $Er^{3+}$ from $^4I_{13/2}$ to $^4I_{15/2}$ near 1550 nm. The line shape of PL spectra has no evident changes with altering the concentrations of Er and Yb. But compared with that of Er(DIOP)$_3$, the PL intensity of $Er_xYb_{(1-x)}(DIOP)_3$ is greatly enhanced, owning to an increased pumping efficiency at 980 nm, because the absorption of $Yb^{3+}$ ions at 980 nm is much stronger than that of $Er^{3+}$ ions, and the $Er^{3+}$ ions can be sensitized by $Yb^{3+}$. The PL intensity does not grow proportionally to the $Er^{3+}$ ions concentration. The inset is the dependence of the PL intensity at 1550 nm on the concentrations of Er and Yb. The explanation for this result is that the total concentrations of Er and Yb in $Er_xYb_{(1-x)}(DIOP)_3$ are constant. Increasing the concentration of $Er^{3+}$ ions, the concentration of $Yb^{3+}$ will be decreased. The optimum concentration of $Er^{3+}$ turns out to be x = 0.107.

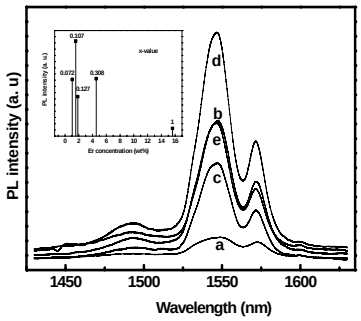


*Fig. 7 PL intensity curves of $Er_xYb_{(1-x)}(DIOP)_3$ with various concentrations of Er and Yb. (a) x = 1 (b) x = 0.308 (c) x = 0.127 (d) x = 0.107 (e) x = 0.072*

## 4. Summary

All $Er_xYb_{(1-x)}(DIOP)_3$ have the same structure. The chemical formula of the complexes is in agreement with $Er_xYb_{(1-x)}[(C_8H_{17}O)_2PO_2]_3$. The $Er_xYb_{(1-x)}(DIOP)_3$ with various concentrations of Er and Yb have a good thermostability. The decomposition temperature range is from about 300 ℃ to 340 ℃. The decomposition temperature is slightly higher with increasing the concentration of Yb. The optimum concentration of $Er^{3+}$ ions in $Er_xYb_{(1-x)}(DIOP)_3$ turns out to be x = 0.107 for obtaining the maximum PL intensity at 1550 nm.

**Acknowledgements**

This work was financially supported by the Natural Science Foundation of Dalian city (2006A10GX052) and the National Natural Science Foundation of China (60577014).

## References

[1] L. H. Slooff, A. Van Blaaderen, A. Polman, G. A. Hebbink, J. W. Hofstraat, J. Appl. Phys. **91**, 3955 (2002).
[2] G. B. Khomutov, I. V. Beresneva, I. V. Bykov, R. V. Gainutdinov, Y. A. Koksharov, Colloids and Surfaces A: Physicochem. Eng. Aspects. **198–200**, 491 (2002).
[3] H. Suzuki, Journal of Photochemistry and Photobiology A: Chemistry. **166**, 155 (2004).
[4] S. Hinojosa, O. Barbosa-Garcia, M.A. Meneses-Nava, J. L. Maldonado,E. de la Rosa-Cruz, G. Ramos-Ortiz, Opt. Mater. **27**, 1839 (2005).
[5] W. H. Wong, K. K. Liu, K. S. Chan, E. Y. B. Pun, J. Crys. Grow. **288**, 100 (2006).
[6] R. Yoshimura, M. Hikita, S. Tomaru, S. Imamura, J. Light. Tec. **16**, 1030 (1998).
[7] W.H. Wong, J. Zhou, E. Y. B. Pun, Appl. Phys. Lett. **78**, 2110 (2001).
[8] E. Kim, S. Y. Cho, D. M. Yeu, S. Y. Shin, Chem. Mater. **17**, 962 (2005).
[9] G. V. Karve, B. Bihari, R. T. Chen, Proc.SPIE. **4282,** 16 (2001).
[10] K. Kuriki, Y. Koike, Chem. Rev. **102**, 2347 (2002).
[11] C. C. Ting, S. Y. Chen, W. F. Hsieh, J. Appl. Phys. **90**, 5564 (2001).
[12] A. Q. Le Quang, J. Zyss, I. Ledoux, V. G. Truong, A. M. Jurdyc, Jacquier, D. H. Le, A. Gibaud, Chem. Phys. **318**, 33 (2005).
[13] J. W. Stouwdam, G. A. Hebbink, J. Huskens, F. C. J. M. Van Veggel, Chem. Mater. **15**, 4604 (2003).
[14] W. H. Wong, E. Y. B. Pun, and K. S. Chan, Appl. Phys. lett. **84**, 176 (2004).
[15] X. J. Wang, M .K. Lei , T.Yang, B. S.Cao, Opt. Mater. **26**, 253 (2004).
[16] D. K. Sardar, J. B. Gruber, B. Zandi, J. A. Hutchinson, C. W. Trussell, J. Appl. Phys. **93**, 2041 (2003).
[17] L. D. da Vila, L. Gomes, L. V. G. Tarelho, S. J. L. Ribeiro, Y. Messadeq, J. Appl. Phys. **93**, 3873 (2003).
[18] J. R. Ferraro, C. Cristallini, I. Fox, J. Inorg. Nucl. Chem. **29**, 139 (1967).
[19] N. M. Karayannis, C. M. Mikulski, J. V. Minkiewicz, L. L. Pytlewski, M. M. Labes. J. Less-Common Metals. **20**, 29 (1970).
[20] C. M. Mikulski, N. M. Karayannis, L. L. Pytlewski. J. Inorg. Nucl. Chem. **34**, 1215 (1972).
[21] A. Z. Ma, L. M. Li, G. F. Zeng, C. Y. Wang, H. Li, Chin. J. Appl. Chem. **6**, 41 (1989).
[22] S. X.. Yao, D. J. Wang, W. J. Zhou, N. Shi, Q. Peng, J. G. Wu, G. X. Xu, Acta Chim. Sinica. **53**, 616 (1995).

*Corresponding author: wang.guimei@yahoo.com.cn

JOURNAL OF OPTOELECTRONICS AND ADVANCED MATERIALS Vol. 9, No. 11, November 2007, p. 3619 - 3623